Synthesis and pre-clinical evaluation of a [^{18}F]fluoromethyl-Tanaproget derivative for imaging of progesterone receptor expression.

Authors:

Shairoz Merchant[1]‡, Louis Allott[2]‡, Laurence Carroll[1], Vickram Tittrea[1], Steven Kealey[3], Timothy H. Witney[1], Philip W. Miller[3], Graham Smith[2] and Eric O. Aboagye[1]

[1]Comprehensive Cancer Imaging Centre, Department of Surgery and Cancer, Imperial College London, Hammersmith Campus, Du Cane Road, London, W12 0NN, UK.

[2]Division of Radiotherapy and Imaging, The Institute of Cancer Research, 123 Old Brompton Road, London, UK

[3]Department of Chemistry, Imperial College London, South Kensington, London, SW7 2AZ, UK

‡ *These authors contributed equally to the work.*

* *Corresponding author.*

ABSTRACT

The estrogen receptor (ER) and progesterone receptor (PR) are over-expressed in ~50% of breast cancer lesions, and used as biomarkers to stratify patients to endocrine therapy. Currently, immunohistochemical (IHC) assessment of these lesions from core-needle biopsy in deep-sited metastases has limitations associated with sampling error and lack of standardization. An alternative solution is positron emission tomography (PET)-based probes, which are inherently quantitative and capable of imaging the entire tumor, including metastases. This work features the synthesis and biological evaluation of a novel fluorinated derivative of Tanaproget, a high affinity non-steroidal PR ligand, as a candidate for imaging PR expression *in vivo*. Radiolabeling of the candidate was achieved in a 15% ± 4 radiochemical yield (non-decay corrected) in one step from [^{18}F]fluoromethyltosylate in 30 min. Cell uptake studies showed a significant difference between the radioligand uptake in PR+ and PR– cell lines; however, *in vivo* imaging was confounded by defluorination hypothesized to occur *via* iminium salt formation. Investigation into high affinity, metabolically stable non-steroidal PR ligands is currently ongoing.

INTRODUCTION

Steroid hormone receptors (SHR) regulate cellular function in healthy tissue, however, over-activation of some SHRs promote the proliferation of hormone-responsive cancer.[1] A definitive example, endogenous estrogen binding to the estrogen receptor (ER), triggers tumor proliferation in 70 – 80% of cases of breast cancer and 33 – 53 % of ovarian cancers.[2-3] Progesterone receptor (PR) expression is regulated by the ER and can consequently behave as a surrogate biomarker to report on ER function. As a result, ER and PR expression have predictive and prognostic importance, allowing patients to be stratified into responders/non-responders of endocrine therapy, the frontline treatment for ER+ tumors.[4] The current gold standard for assessment of ER/PR expression is *ex vivo* immunohistochemistry (IHC) which is prone to misrepresent heterogeneity of receptor expression.[5-7] Positron emission tomography (PET) may overcome the limitations of IHC by quantifying receptor expression in metastatic lesions where biopsy sampling is challenging, while also accounting for heterogeneous receptor expression in primary disease. The use of the ER-targeted radioligand, 16α-[^{18}F]fluoro-17β-estradiol ([^{18}F]FES), shown in Figure 1, has been successful in many clinical trials involving primary and metastatic breast cancer.[8-18] Further integration of [^{18}F]FES-PET into routine clinical experience is hampered by rapid metabolism and the difficulty of imaging patients receiving endocrine therapy owing to competition for ER between the radioligand and the therapeutic agent.[19] This has prompted investigation into PR targeted radioligands to report on the presence of a functional ER pathway. 21-[^{18}F]Fluorofuranyl-norprogesterone ([^{18}F]FFNP) (Figure 1) has been used successfully to image PR expression in a clinical trial, as well as pre-clinical studies to determine if [^{18}F]FFNP could report on response to endocrine therapy.[20-22]Although studies into [^{18}F]FFNP as a radioligand for imaging PR expression have been promising, its physicochemical properties, e.g., high LogP associated with the steroidal structure of the ligand may compromise specificity for PR binding.

Tanaproget (Figure 1) is a high affinity, highly specific, non-steroidal PR agonist (EC_{50} = 0.15 nM) developed by Wyeth as an orally bioavailable contraceptive.[23] Tanaproget derivatives have previously been investigated for use as radioligands where derivatization at the R_2-position provided racemic [^{18}F]fluoropropyl-tanaproget([^{18}F]FPTP) (Figure 1), which showed promising results in preliminary *in vivo* studies.[24-25] Subsequently, [^{18}F]FPTP was synthesized in a 5% yield (decay corrected) with a specific activity >20 GBq/μmol; tissue biodistribution was evaluated in immature estrogen-primed female rats and proved to exhibit favorable target distribution with high uptake in uterus and reduced uptake in bone compared to [^{18}F]FFNP.[25] [^{18}F]FPTP was evaluated as a racemic mixture despite computational studies showing that the *S*-enantiomer was likely to adopt the lowest energy conformation in the PR ligand-binding domain; therefore, the racemic mixture is likely to contain two ligands exhibiting different affinities.[24] Structures of ^{18}F-labeled PR compounds in the literature are

shown in Figure 1A.[24-27] The relative binding affinities (RBA) of Tanaproget and related ^{18}F-labelled scaffolds are shown in Figure 1B.

A.

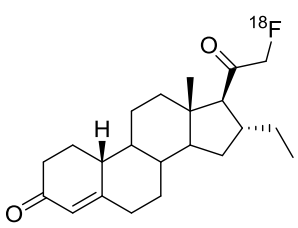

[^{18}F]FENP

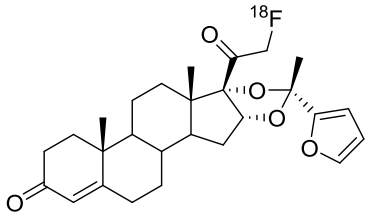

[^{18}F]FFNP

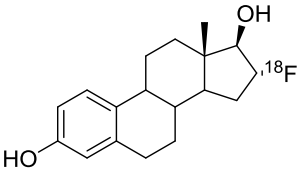

[^{18}F]FES

B.

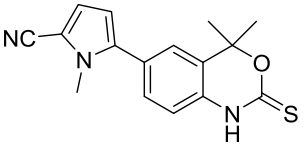

Tanaproget

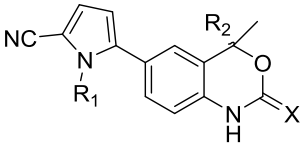

Tanaproget core scaffold

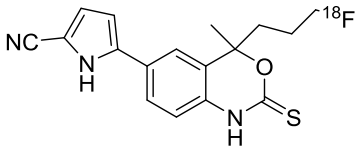

[^{18}F]FPTP

Fluoroalkyl derivitization at R_1	RBA (R5020 = 100)
-CH_3	151 ± 39
-CH_2CH_2F	18.5 ± 5.2
-$CH_2CH_2CH_2F$	0.99 ± 0.28
[^{18}F]FPTP	189

Figure 1. A. Structures of ^{18}F-labelled PR compounds in the literature.[22-23, 25-26] **B.** Relative Binding Affnity (RBA) of fluorinated Tanaproget derivatives obtained from competitive PR assays where the standard progestin R5020 is given a value of 100; R_1& R_2 = fluoroalkyl substituents; X = O or S.[23]

In the same report, Zhou *et al.* also investigated fluoroalkyl- substitution at the *N*-pyrrole position where derivatization would not introduce a chiral center. Fluoroethyl and fluoropropyl derivatives were synthesized and evaluated for PR binding affinity (data summarized in Figure 1B).[24] The affinity data reported by Zhou and co-workers indicates an inverse relationship between fluoroalkyl chain length and PR binding affinity. Based on this observed trend we reasoned that N-fluoromethyl-alkylation could provide a radioligand with improved PR binding affinity. [^{18}F]Fluoromethyltosylate is a versatile prosthetic group for which our group recently published an automated, cassette based and HPLC free GMP compatible radiosynthesis.[28] Further motivation to explore radiolabeling at the *N*-pyrrole position included the opportunity to conserve the gem-dimethyl substitution at the R_2-position on the core scaffold, eliminating the chiral center formed in [^{18}F]FPTP. Removing chirality from the radioligand a) precludes competition between enantiomers exhibiting different affinities for PR, which may have a confounding effect on receptor quantification and b) also precludes any

requirement for chiral purification and QC analysis. Furthermore, analysis of the SAR from the development of Tanaproget suggested that the thiocarbamate is involved in determining biological profile of the ligand (agonist or antagonist) but does not assist in the formation of important hydrogen bonds to aid ligand binding. This observation, combined with evaluation of the available reports from the Wyeth group, furnished the conclusion that the thiocarbonyl was not strictly necessary for high PR binding affinity but rather "flipped" agents from antagonist to agonist, although this is not a strictly observed rule of thumb.[23] As PET uses concentrations of radioligand that typically obey the tracer principle, biological profile (agonist/antagonist) of a lead candidate is deprioritized in favor of other desirable design properties, therefore we hypothesized that the thiocarbonyl may be dispensable in favor of a more synthetically accessible simple carbamate. Removal of the thiocarbamate functionality was considered favorable as its presence could hinder reaction progress when electrophilic reactive groups (e.g. alkylating agents) are used for the radiolabeling step; carbamates are less susceptible to electrophilic attack. Furthermore, replacement of the thiocarbamate with a simple carbamate would eliminate the need to convert the carbonyl to the thiocarbonyl post-radiolabeling; this has previously been achieved by using Lawessons reagent as reported by Zhou *et al.* in the radiosynthesis [^{18}F]FPTP.[25] Herein we describe the synthesis and evaluation of a Tanaproget derivative that features facile access to a radiolabeling precursor and a simple radiolabeling strategy.

RESULTS AND DISCUSSION

Synthesis of the reference compound (6). The reference compound **6** was tested for PR potency to verify our hypothesis concerning probe design (prior to any radiolabeling); chemical methodology is described in Scheme 1. 6-Bromo-4,4-dimethyl-1,4-dihydrobenzo[d][1,3]oxin-2-one **2**, was coupled with *N*-boc-pyrrole boronic acid using a palladium-catalyzed Suzuki reaction to give **3** in a moderate yield of 47%. Subsequent cyanation of the pyrrole at the 5-position using chlorosulfonylisocyanate (CSI) and subsequent thermolysis to remove the protecting group gave precursor **5** efficiently in 31% over two steps. Alkylation of the *N*-H pyrrole nitrogen with fluorobromomethane gave the desired compound **6** in a yield of 19% under basic conditions in DMF.

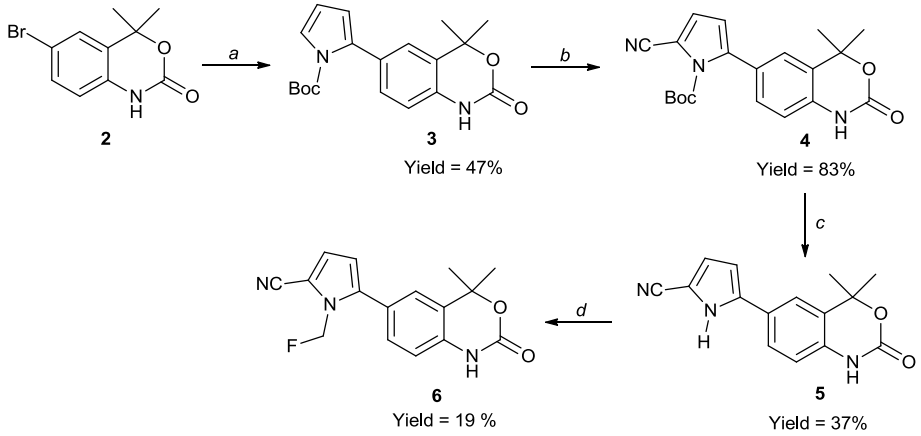

Scheme 1. Preparation of reference compound 6. (*a*) N-boc pyrrole boronic acid, $Pd(PPh_3)_4$, K_2CO_3, EtOH, toluene, H_2O, 80°C, 16 h. (*b*) CSI, THF, -78 °C, 90 min, then DMF, RT, 16 h. (*c*) N_2, 170 °C, 20 min. (*d*) fluorobromomethane, K_2CO_3, DMF, RT, 16 h.

Radiolabelling compound 6. The prosthetic group [^{18}F]fluoromethyltosylate has been routinely synthesized within our laboratory starting from methylene ditosylate.[28] From there, coupling to the nitrogen on the pyrrole ring was achieved using K_2CO_3 in DMF at 150 °C in an isolated radiochemical yield of 15% ± 4 (n = 20, non-decay corrected) (**Scheme 2**). Temperatures of 25 °C, 90 °C and 110 °C were all studied, but gave minimal radiochemical incorporation (<1% by analytical HPLC), whilst the reaction did not proceed as cleanly without the presence of K_2CO_3 as a base, with up to two other radiochemical peaks noted in the absence of K_2CO_3. The product was isolated using semi-preparative HPLC and reformulated into ethanol, before being diluted down using saline solution to less than 5% ethanol content in the formulated mixture. Specific activity was routinely found to be between 10 and 20 GBq. Radiochemical stability of > 99% was found upto 4 hours in ethanol and saline independently.

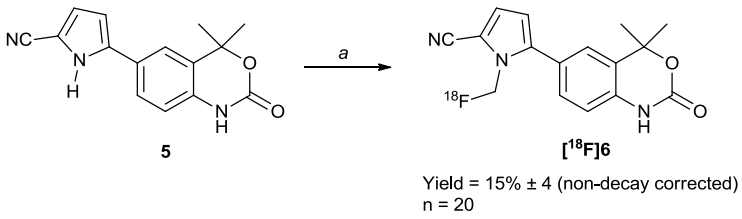

Scheme 2. Radiolabelling of precursor **5**. (*a*) [^{18}F]fluoromethyltosylate, K_2CO_3, DMF, 150°C, 30 min.

PR receptor interaction. The cell-free PolarScreen™ PR competitor assay was used to determine the half-maximal PR competitive binding affinity, IC_{50}, and therefore the relative binding affinity (RBA; relative to progesterone). Compound **6** had an IC_{50} of 29.9 ± 10.2 nM (**Figure 2**); the RBA of **6** was 127.5% when compared directly to progesterone. Taken together, the affinity data demonstrate that compound **6** has high affinity for PR and is suitable for further evaluation as a PET probe. It should be noted, however, that at low concentrations, progesterone had non-linearly lower affinity for PR. This may be a relevant consideration when compound **6** is used at the typical low concentrations for PET imaging against a background of variable progesterone levels in nude and haired laboratory mice (2-22 ng/mL).

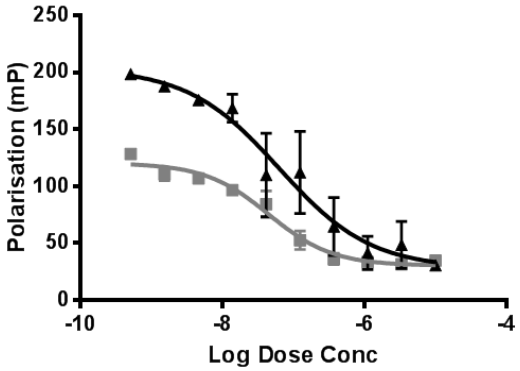

Figure 2. Determination of the relative PR-binding using a cell-free fluorescence polarization assay. Progesterone (filled triangles) and compound **6** (filled squares) were tested.

Binding specificity. Compound **6** was studied for cross-reactivity to other steroid receptors including GR, AR and ER using luciferase reporter assays (Figure 3). Dexamethasone, a GR ligand exhibited high luciferase activity in keeping with activation of GR reporter; MPA (medroxyprogesterone acetate), a potent progesterone agonist, had minimal GR activity while compound **6** showed negligible activation of GR (Figure 3). DHT interacted with AR with ~10-15-fold activation at concentrations up to 1 µM. MPA and compound **6** increased AR activation by ~2.5-fold at 1 µM. In the ER luciferase

reporter assay, compound **6** and MPA activated the receptor by approximately 2-fold less than estrogen (**Figure 4**). These assays demonstrated high specificity of compound **6** for PR (low non-specific interaction with related receptors).

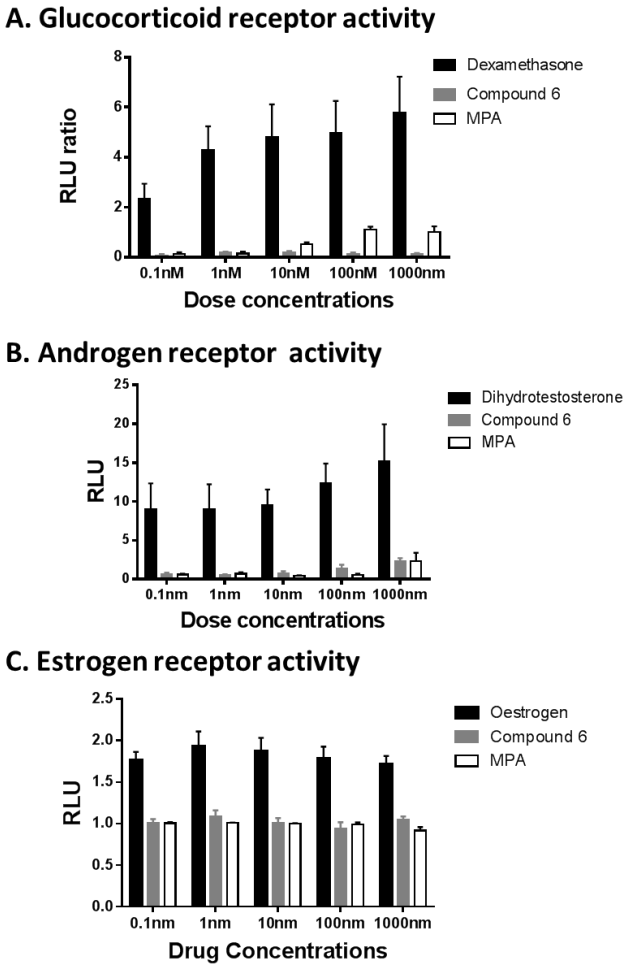

Figure 3. Specificity of binding. Compound **6** together with relevant controls were tested to determine specificity for **A**. GR, **B.** AR or **C.** ER. MPA, Medroxyprogesterone acetate. RLU, Relative light units using firefly luciferase; in the case of A, the RLU of firefly luciferase to that of renilla luciferase was determined (thus, RLU ratio).

***In vitro* cell uptake study.** Subsequently, *in vitro* uptake experiments were carried out using **[^{18}F]6** in three breast cancer cell lines – MCF7, MDA-MB-231 and T47D - with different PR expression (Figure 4A). Uptake of **[^{18}F]6** correlated with PR expression determined by western blotting. T47D cells showed highest PR-α and PR-β expression followed by MCF-7; PR expression was undetectable in MDA-MB-231 cells. The uptake of **[^{18}F]6** was determined in these cell lines under estrogen-induced conditions. The uptake of **[^{18}F]6** (Figure 4B) was associated with PR expression determined from the western blots. Of note, **[^{18}F]6** was non-negligible in MDA-MB-231 cells demonstrating some degree of non-specific interaction in this PR negative cell line. To further verify specificity, we

incubated T47D cells with varying levels of progesterone to block the receptor prior to addition of **[^{18}F]6** (**Figure 4C**). By progressively increasing the dose of progesterone up to 10 μM, uptake of **[^{18}F]6** decreased to one third of its original value, demonstrating that **[^{18}F]6** uptake was broadly specific to the PR ligand binding.

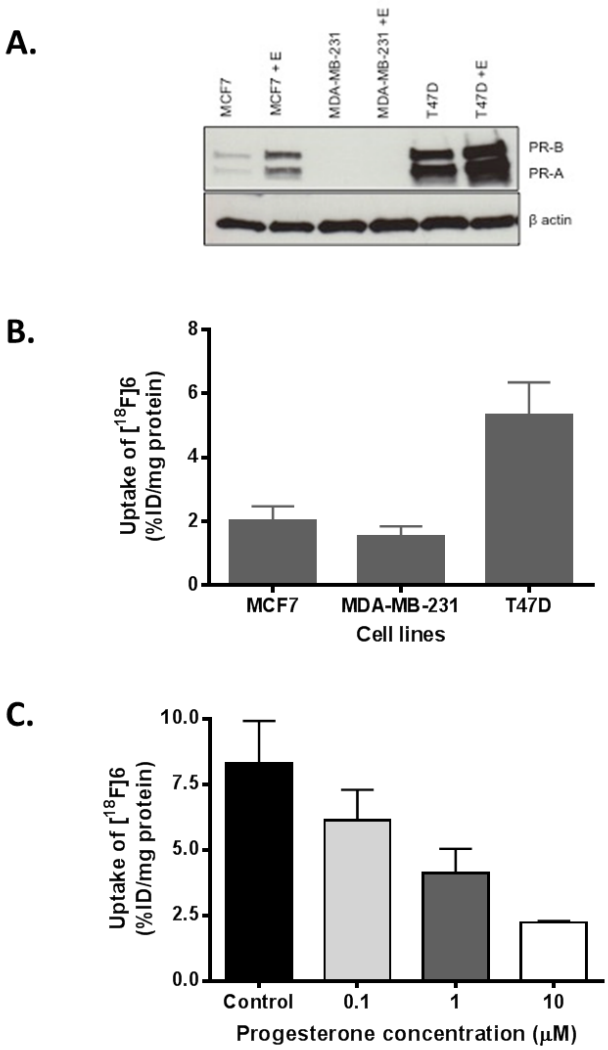

Figure 4. Uptake of **[^{18}F]6** in cells with varying PR expression. **A.** PR expression in the presence or absence of estrogen (E) as determined by western blot. β-actin was used as load control. **B.** Uptake of [^{18}F]**6** in the different cell lines. **C.** Blocking of **[^{18}F]6** uptake in T47D cells pre-treated with varying concentrations of progesterone.

As further validation to understand the context of binding (antagonist vs agonist), we synthesized [^{11}C]tanaproget according to our previously published methodology[29] (Figure 5A) and performed uptake studies in PR positive and negative cells. The magnitude of uptake of [^{11}C]tanaproget in the cells was broadly similar to that seen with **[^{18}F]6** (Figure 5B). Surprisingly, blocking with progesterone or unlabeled tanaproget led to an increase rather than a decrease in [^{11}C]tanaproget-

uptake. This led us to question whether uptake of [^{11}C]tanaproget was modulated by Multi-Drug Resistance (MDR) protein interaction and hypothesise that self-blocking could be abolished when MDR mechanism is inhibited/saturated with a modulator. Treatment of cells with verapamil, a P-gp inhibitor, increased uptake by approximately 30%, supporting a role for MDR (Figure 5C). Similar increases in calcein (an MDR substrate) uptake in the cell lines following pre-treatment with progesterone or tanaproget corroborated the radioligand uptake studies (Figure 6D). It is important to note that a >15-fold higher concentration of verapamil was required to increase [^{11}C]tanaproget uptake compared to unlabeled tanaproget or progesterone. The specific reason for this is not known but could be due to the a more efficient inhibition of P-gp by progesterone compared to verapamil reported in some studies, differential specificity of [^{11}C]tanaproget for multidrug resistance proteins [P-glycoprotein (P-gp; MDR1), multidrug resistance-associated proteins (MRP1, MRP2, MRP3, MRP4, and MRP5), and breast cancer resistance protein (BCRP)] or differential expression of these proteins in MDA-MB-231 and T-47D cells.[30]

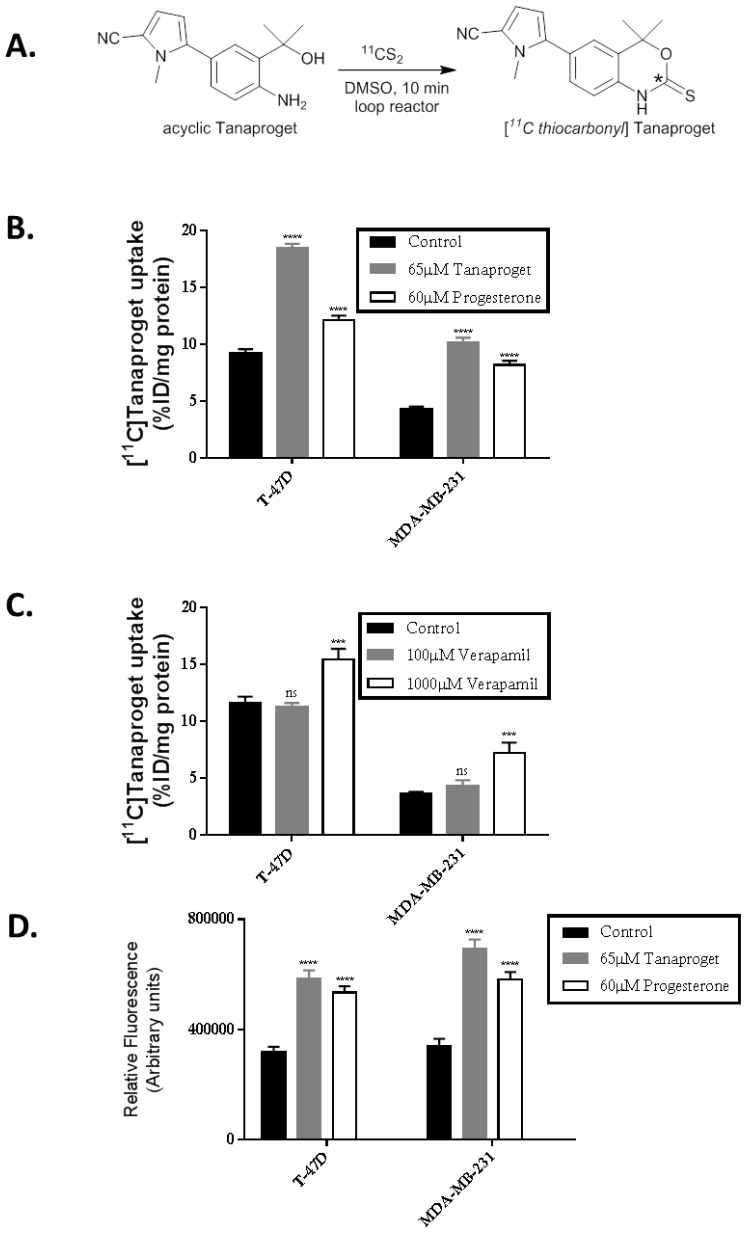

Figure 5. Uptake of isotopically labelled [^{11}C]tanaproget in cells. A. Synthesis of [^{11}C]tanaproget. **B.** Uptake of [^{11}C]tanaproget in PR-proficient and PR-deficient cell lines, in the presence or absence of blocking dose of tanaproget or progesterone. C. Effect of verapamil on [^{11}C]tanaproget uptake. D. Effect of the same chemical modulators in used C on uptake of calcein-AM (effect on multidrug resistance protein interaction).

***In* vivo evaluation of [^{18}F]6.** *In vitro* experiments indicated the potential for **[^{18}F]6** to be a candidate radioligand for PR imaging; therefore, *in vivo* imaging was studied in mice bearing T47D xenografts. Summed images 30-60 minutes post-injection from 60 minute dynamic PET scans using **[^{18}F]6** and [^{18}F]FDG are shown in Figure 6. These indicate a viable tumor ([^{18}F]FDG scan) but marginal selective uptake for **[^{18}F]6**. This is further confirmed by comparison of uptake in tumor for **[^{18}F]6** and

[^{18}F]FDG shown in Figure 6C. The time activity curve of **[^{18}F]6** (Figure 6B) showed a gradual rise in bone localization over the course of the imaging sequence, almost trebling between 5 and 60 min. The maximal uptake in bone from biodistribution (γ-counting) studies was 17.5 % ID/g at 60 min (Figure 7A). This suggest *in vivo* defluorination of **[^{18}F]6**. Liver uptake was also high (20.3 % ID/g) (Figure 7A).

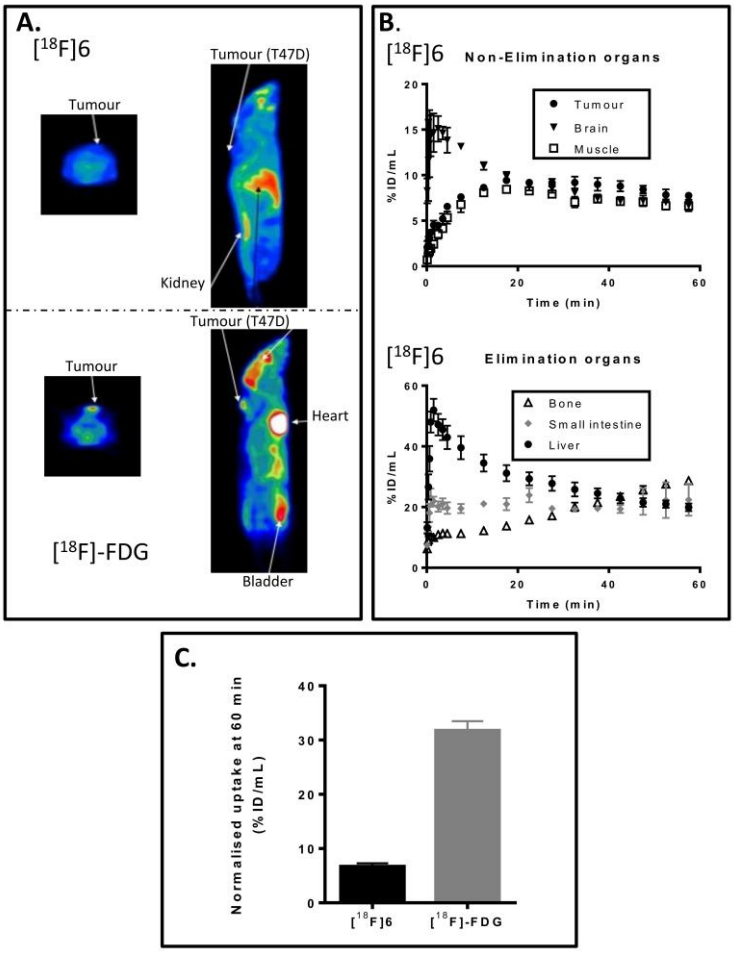

Figure 6. Imaging studies with **[^{18}F]6** and [^{18}F]FDG. **A**. Axial and sagittal PET images of **[^{18}F]6** and [^{18}F]FDG 30-60 post-injection. **B.** Time activity curves of both radiotracers in different organs and tumor N=3 animals. **C.** Quantitative comparison of tumor uptake of **[^{18}F]6** and [^{18}F]FDG (N=3 animals per group; $p < 0.0001$).

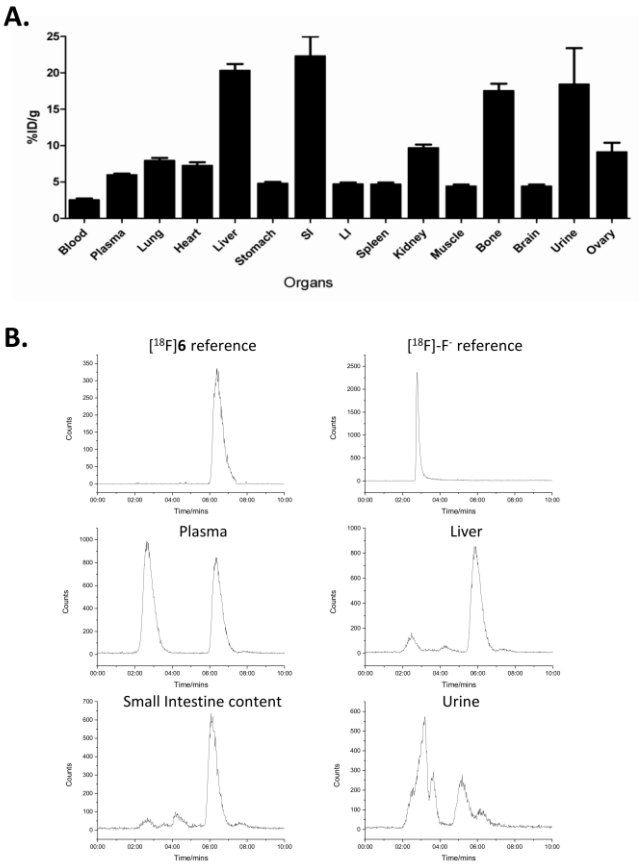

Figure 7. Normal tissue biodistribution and *in vivo* metabolism of **[^{18}F]6**. **A**. Biodistribution of **[^{18}F]6** in different organs at 60 min after intravenous injection. **B.** Radio-HPLC chromatograms of **[^{18}F]6** in different tissues at 60 min post intravenous injection.

Defluorination assay. To confirm the hypothesis that bone uptake was a result of **[^{18}F]6** defluorination, we carried out a metabolite assay by taking fractions at 60 min of selected organs and analyzing *via* radio-HPLC (Figure 7). In each sample, apart from the reference compound (parent R_t = 5.5 minutes), [^{18}F]fluoride (R_t = 2 minutes, by comparison with [^{18}F]fluoride direct from the cyclotron under the same chromatographic conditions), and a second metabolite (R_t = 4 minutes) were seen (**Figure 7B**). In particular, circulating plasma contained more than 50% of the activity as [^{18}F]fluoride at 60 min, this supports the notion that defluorination correlates with bone uptake. A summary of the proportions of radio-analytes are shown in **Table 1**.

Sample (n = 3)	[^{18}F]Fluoride/%	Metabolite/%	[^{18}F]6/%
[^{18}F]6 reference	-	-	99 ± 1
[^{18}F]Fluoride reference	99 ± 1		
Urine	65 ± 3	25 ± 2	10 ± 4
Plasma	55 ± 5	-	45 ± 5
Liver	13 ± 3	5 ± 1	82 ± 2
Small intestine contents	8 ± 4	11 ± 4	81 ± 2

Table 1. Fraction of **[^{18}F]6** remaining after 60 min (n=3 for each sample).

Examining previously described work, Jehangir *et al* had reported the formation of highly reactive iminium salt from 1-fluoro-*N*,*N*-dimethylmethanamine which is analogous to **[^{18}F]6**, with a similar defluorination mechanism possible (Scheme 3A).[31] Although no fluoride was ever seen in a formulated sample of **[^{18}F]6** after 4 hours, it seems likely that any number of factors present *in vivo*, such as variations in pH above and below 7, could push the mechanism to a dissociated [^{18}F]fluoride as shown in Scheme 3.[31]

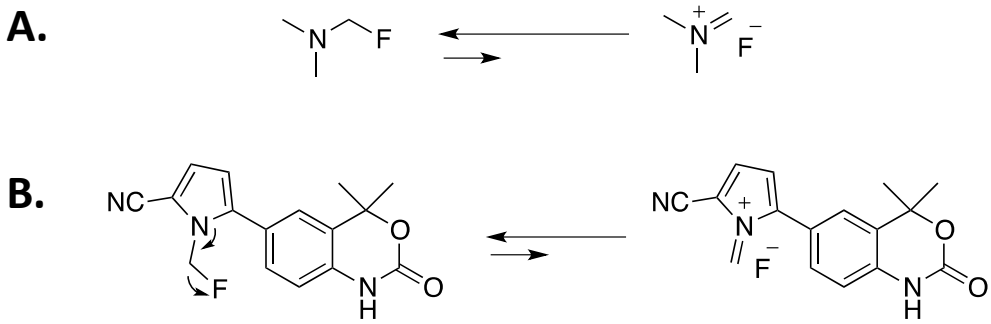

Scheme 3. A) Defluorination of 1-fluoro-*N*,*N*-dimethylmethanamine.[30] **B**) Hypothesized mechanism for the defluorination of compound **[^{18}F]6** by iminium salt formation.

DISCUSSION

Steroid-derived PET imaging agents such as [^{18}F]FDHT (AR), [^{18}F]FES (ER) and [^{18}F]FFNP (PR) continue to generate interest for patient stratification to inform treatment regimen planning. Four

decades of research into SHR imaging agents have resulted in the formulation of important criteria for developing successful imaging agents. The rate of attrition of SHR imaging candidates is attributed to poor receptor specificity, unfavorable biodistribution and rapid metabolism, characteristics that can generally be associated with steroidal compounds. More recently, investigation of non-steroidal SHR imaging agents to circumvent these negative characteristics have identified promising compounds particularly in the case of PR targeted radioligands.[32] Lee *et al.* (2010) synthesized tanaproget derivative [^{18}F]FPTP which has shown potential by successfully imaging PR expression *in vivo*. Although [^{18}F]FPTP is a promising candidate radioligand, we proposed an alternative derivative (**[^{18}F]6**) for investigation.

We speculated that **[^{18}F]6** would exhibit a high affinity for PR based on SAR observations in the literature.[24] The synthesis of the precursor for **[^{18}F]6** involved relatively a five step synthesis with an overall yield of 6%. The radiolabeling procedure of **[^{18}F]6** was simplified compared to [^{18}F]FPTP as our design criteria removed the requirement of further structural modifications post-labeling. We postulated that the agonist/antagonist binding mode for the imaging agent could be de-prioritized because concentration of compound administered would be too low to perturb the biological system; based on this assumption, converting **[^{18}F]6** from the carbamate to thio-carbamate was not necessary. Radioligand **[^{18}F]6** was synthesized in 120 min from end of bombardment (EOB) in a one-step procedure from [^{18}F]fluoromethyltosylate which was faster than [^{18}F]FPTP, synthesized in 140 min from EOB. The relative simplicity of the radiochemistry of **[^{18}F]6** was considered to be advantageous if the procedure was to be automated for routine pre-clinical/clinical production; [^{18}F]FPTP required a more challenging procedure due to post-labeling conversions and as a result, automation of the radiosynthesis would be challenging.

Compound **[^{18}F]6** was shown to bind the PR with a low nanomolar affinity and exhibited negligible cross-reactivity to the GR even at 100-fold concentration of ligand. *In vitro* evaluation of **[^{18}F]6** was successful in showing significant uptake in PR+ cells that could be blocked with substrates selective for the PR ligand binding domain (LBD). This confirmed that **[^{18}F]6** binds the same receptor LBD as known steroidal progestins and not an allosteric site. These were encouraging results as they supported the assumption of deprioritizing binding profile in favor of more important characteristics.

In vivo performance of **[^{18}F]6** was investigated in both T47D xenograft bearing mice and normal female mice; however, tumor uptake of **[^{18}F]6** was poor which was likely to be the result of insufficient metabolic stability over the imaging time-frame. Extensive defluorination (17.5 % ID/g in bone) was observed at 60 min, which we propose is facilitated by iminium salt formation (Scheme 3). Furthermore, it may be possible that the low nanomolar affinity of **[^{18}F]6** was sufficient to observe selective uptake in an *in vitro* cell model but may be insufficient for imaging *in vivo* PR expression. Most steroid-based PR ligands exhibit sub-nanomolar affinity and it may be the case that, similarly

high affinity is required for non-steroidal imaging ligands. An avenue of interest for further research is the development of higher affinity PR ligands, which could potentially be achieved using a medicinal chemistry based fragment screening campaign. The specific activity of **[^{18}F]6** was estimated to be about 10 GBq/μmol. In a mouse weighing 20g this would equate to a dose of cold **[^{19}F]6** estimated at ~2.8 μg/kg, well below the level of a therapeutic dose which would be expected in the range of 1 mg/kg or above. Therefore, the imaging protocol complied with the concept of the "tracer principle" and the mode of binding (agonist or antagonist) could be discounted as a factor in *in vivo* performance of the **[^{18}F]6**.

Tanaproget served as a useful starting point for developing PR imaging agents investigated herein and previously, however, we have shown that even with careful consideration when derivatizing the structure, deviation from sub-nanomolar affinity and poor metabolic stability can hinder the development of an effective *in vivo* imaging agent. Attracted by the sub-nanomolar affinity of tanaproget, we decided to investigate carbon-11 radiolabeled Tanaproget, accessed *via* a novel [^{11}C]carbon disulfide pathway reported elsewhere.[29] Given the high affinity of tanaproget for PR we were surprised by the poor performance of this agent in cell-uptake models. Inhibition of P-gp using verapamil partially reversed this phenomenon, indicating a role for cellular efflux proteins in localization of [^{11}C]tanaproget. This therefore highlights another important consideration for the future development of non-steroidal PR imaging agents.

It is prudent to evaluate the limitations of **[^{18}F]6** and how these characteristics can influence the future design of non-steroidal PR ligands. From analysis of a previous study by Zhou and the results from this study, it is apparent that a number of design criteria are applicable to non-steroidal PR imaging probes. High PR selectivity (at least 100-fold over related SHRs) is of paramount importance. Successful clinical translation of a PR-targeted radioligand is dependent on accurate quantification of receptor expression to stratify patients and therefore cross-reactivity to other SHRs would confound imaging results. Radioligand **[^{18}F]6** was shown to be highly selective for PR over a panel of SHRs (AR, GR, ER). Sub-nanomolar affinity for PR is an important consideration; although **[^{18}F]6** was able to specifically detect PR expression *in vitro*, the presence of circulating endogenous steroid hormones *in vivo* may out-compete radioligands of lower affinity. Although **[^{18}F]6** did not exhibit sub-nanomolar affinity, it performed well in *in vitro* binding assays. We are unable to confidently conclude if **[^{18}F]6** was of appropriate affinity to image PR due to fast metabolism of the radioligand. It should be noted that sub-nanomolar affinity is a high-ranking priority in PR ligand design but should not be used as a metric for extrapolating success of imaging PR *in vivo*. Radioligand [^{11}C]tanaproget, is a non-steroidal PR ligand that exhibits sub-nanomolar affinity yet was had limited selectivity for PR *in vitro*. We have shown the importance of ensuring PR ligands are poor substrates for MDR proteins. The role of sex-hormone binding protein (SHBP) in the pharmacokinetics of steroidal SHR ligands

(e.g. [^{18}F]FES, [^{18}F]FDHT) has long been studied; detailed evaluation of the role of MDR proteins may provide insight to influence ligand design going forward. One assumption we used for PR ligand design was the deprioritization of biological profile (agonist/antagonist binding mode). In this study, we showed that *in vitro* uptake of **[^{18}F]6** was not influenced by biological profile of the radioligand. A high priority for SHR imaging remains to be specific activity; at 10 GBq/μmol **[^{18}F]6**, may not be high enough to image PR *in vivo*. In addition, the standard design criteria that are generally applicable in new PET probe design remain relevant.[33-34]

In summary, **[^{18}F]6** was unsuccessful at imaging *in vivo* PR due to rapid metabolism, however, it is important to stress that the success of **[^{18}F]6** did not hinge on this factor alone and potentially, may have been confounded by other factors despite rapid metabolism. Exhibiting a 10-fold lower affinity than the literature suggests and an average specific activity, **[^{18}F]6** may not have had the necessary characteristics for imaging *in vivo* PR, despite its success in *in vitro* studies.

CONCLUSION

In conclusion, we have examined the synthesis of a radiotracer **[^{18}F]6** based upon the derivatization of tanaproget, and have shown that **[^{18}F]6** has good uptake *in vitro* for cell lines expressing PR, demonstrating that the uptake is specific for PR. Unfortunately, **[^{18}F]6** showed poor metabolic stability, with overriding bone uptake seen by the end of the imaging protocol, suggesting that this compound is not suitable for *in vivo* imaging in mice, and unless metabolism can be demonstrated to be species specific, will predict non-suitability in humans. Work is currently on-going to explore possible variations on the structure to give a more promising long-term candidate for *in vivo* PR imaging.

EXPERIMENTAL PROCEDURES

Radiosynthesis of [^{18}F]6. [^{18}F]Fluoromethyltosylate was synthesized as previously described, and was used after SPE trapping and elution with MeCN (200 μL).[28] [^{18}F]Fluoromethyltosylate (on average, approximately 2 GBq starting from 3 GBq before drying) was added to 100 μL of dry DMF containing compound **5** (5 mg) and K_2CO_3 (5 mg). The reaction mixture was heated at 150 °C for 30 minutes before being cooled and diluted with 8 mL of 2:3 H_2O:MeCN and injected on semi-preparative HPLC (Phenomenex Luna C18, 250 × 10, 2:3 H_2O:MeCN, 3 mL/min). The labelled product **6** was collected (R_t = 9 min) and subsequently reformulated using tC18 light SPE cartridge (prepared with 2 mL EtOH and 5 mL H_2O) after being diluted with 10 mL of H_2O. **[^{18}F]6** was eluted from the tC18 cartridge in EtOH (5 x 100 μL fractions) with the most concentrated fractions being 3 and 4, with a 10% (non-decay corrected) yield starting from [^{18}F]fluoromethyltosylate. Analytical radioHPLC was carried out to confirm the compound (Gemini C18, 150 × 4.6, 1:1 H_2O:MeCN, 1 mL/min) with a R_t of 5.5 minutes.

ASSOCIATED CONTENT

Supporting Information. The supporting information features previously reported synthetic chemistry methods and analytical data ($^{1}H/^{13}C$ NMR and ESI-HRMS). The material is available free of charge on the ACS Publication website http://pubs.acs.org

ACKNOWLEDGEMENTS

This work was funded by Cancer Research UK & Engineering and Physical Sciences Research Council (in association with the Medical Research Council and Department of Health (England)) grant C2536/A10337 and Cancer Research UK grant C2536/A16584. Louis Allott and Graham Smith acknowledge support from the Cancer Research UK Cancer Imaging Centre (grant no. C1060/A16464). Vickram Tittrea acknowledges support from the Medical Research Council (grant no. MR/J015881/1).

ETHICAL APPROVAL

Animal studies were performed in accordance with the UK Animal (Scientific Procedures) Act 1986 and National Cancer Research Institute guidelines [28] within a Designated Establishment under the 1986 Act (the Central Biomedical Services Unit at Imperial College London). The work was done under UK Home Office Project Licence 70/7113. Mice were maintained in individually ventilated cages with environmental enrichment. Procedures were performed with anaesthetic and post-operative analgesics. The studies were designed to detect radiotracer distribution kinetics.[35]

ABREVIATIONS

AR, androgen receptor; BCA, bicinchoninic acid; CSI, chlorosulfonylisocyanate; DMEM, Dulbecco's Modified Eagle's Medium; E2, estradiol; ER, estrogen receptor; [^{18}F]FDG, 2-deoxy-2-[^{18}F]fluoro-D-glucose; [^{18}F]FES, 16α-[^{18}F]fluoro-17β-estradiol; [^{18}F]FFNP,21-[^{18}F]Fluorofuranyl-norprogesterone; [^{18}F]FPTP, [^{18}F]Fluoropropyl-Tanaproget; GR, glucorticoid receptor; IHC, immunohistochemical MPA, medroxyprogesterone acetate; PR, progesterone receptor; pRLTK, thymidine kinase promoter-Renilla luciferase reporter plasmid; R5020, promegestone; RLU, relative light units; RBA, relative binding affinity; RIPA, radio-immunoprecipitation assay; SAR, structure activity relationship; SCID, severe combined immunodeficiency;

REFERENCES

1. McGuire, W. L., Steroid Receptors in Human Breast Cancer. *Cancer Res.* **1978,** *38*, 4289-4291.

2. Harding, M.; Cowan, S.; Hole, D.; Cassidy, L.; Kitchener, H.; Davis, J.; Leake, R., Estrogen and progesterone receptors in ovarian cancer. *Cancer* **1990,** *65* (3), 486-91.

3. Keen, J. C.; Davidson, N. E., The biology of breast carcinoma. *Cancer* **2003,** *97* (3 Suppl), 825-33.

4. Osborne, C. K.; Yochmowitz, M. G.; Knight, W. A., 3rd; McGuire, W. L., The value of estrogen and progesterone receptors in the treatment of breast cancer. *Cancer* **1980,** *46*, 2884-8.

5. Harvey, J. M.; Clark, G. M.; Osborne, C. K.; Allred, D. C., Estrogen receptor status by immunohistochemistry is superior to the ligand-binding assay for predicting response to adjuvant endocrine therapy in breast cancer. *J. Clin. Oncol.* **1999,** *17* (5), 1474-81.

6. DeSombre, E. R.; Thorpe, S. M.; Rose, C.; Blough, R. R.; Andersen, K. W.; Rasmussen, B. B.; King, W. J., Prognostic usefulness of estrogen receptor immunocytochemical assays for human breast cancer. *Cancer Res.* **1986,** *46*, 4256s-4264s.

7. Hammond, M. E.; Hayes, D. F.; Dowsett, M.; Allred, D. C.; Hagerty, K. L.; Badve, S.; Fitzgibbons, P. L.; Francis, G.; Goldstein, N. S.; Hayes, M.; Hicks, D. G.; Lester, S.; Love, R.; Mangu, P. B.; McShane, L.; Miller, K.; Osborne, C. K.; Paik, S.; Perlmutter, J.; Rhodes, A.; Sasano, H.; Schwartz, J. N.; Sweep, F. C.; Taube, S.; Torlakovic, E. E.; Valenstein, P.; Viale, G.; Visscher, D.; Wheeler, T.; Williams, R. B.; Wittliff, J. L.; Wolff, A. C., American Society of Clinical Oncology/College of American Pathologists guideline recommendations for immunohistochemical testing of estrogen and progesterone receptors in breast cancer (unabridged version). *Arch. Patho.l Lab. Med.* **2010,** *134* (7), 48-72.

8. Mintun, M. A.; Welch, M. J.; Siegel, B. A.; Mathias, C. J.; Brodack, J. W.; McGuire, A. H.; Katzenellenbogen, J. A., Breast cancer: PET imaging of estrogen receptors. *Radiology* **1988,** *169* (1), 45-8.

9. McGuire, A. H.; Dehdashti, F.; Siegel, B. A.; Lyss, A. P.; Brodack, J. W.; Mathias, C. J.; Mintun, M. A.; Katzenellenbogen, J. A.; Welch, M. J., Positron tomographic assessment of 16 alpha-[^{18}F] fluoro-17 beta-estradiol uptake in metastatic breast carcinoma. *J. Nucl. Med.* **1991,** *32* (8), 1526-31.

10. Linden, H. M.; Stekhova, S. A.; Link, J. M.; Gralow, J. R.; Livingston, R. B.; Ellis, G. K.; Petra, P. H.; Peterson, L. M.; Schubert, E. K.; Dunnwald, L. K.; Krohn, K. A.; Mankoff, D. A., Quantitative fluoroestradiol positron emission tomography imaging predicts response to endocrine treatment in breast cancer. *J. Clin. Oncol.* **2006,** *24* (18), 2793-9.

11. Dehdashti, F.; Mortimer, J.; Trinkaus, K.; Naughton, M.; Ellis, M.; Katzenellenbogen, J.; Welch, M.; Siegel, B., PET-based estradiol challenge as a predictive biomarker of response to endocrine therapy in women with estrogen-receptor-positive breast cancer. *Breast Cancer Res. Treat.* **2009,** *113* (3), 509-517.

12. Tsujikawa, T.; Yoshida, Y.; Kudo, T.; Kiyono, Y.; Kurokawa, T.; Kobayashi, M.; Tsuchida, T.; Fujibayashi, Y.; Kotsuji, F.; Okazawa, H., Functional images reflect aggressiveness of endometrial

carcinoma: estrogen receptor expression combined with ^{18}F-FDG PET. *J. Nucl. Med.* **2009,** *50* (10), 1598-604.

13. Tsujikawa, T.; Yoshida, Y.; Kiyono, Y.; Kurokawa, T.; Kudo, T.; Fujibayashi, Y.; Kotsuji, F.; Okazawa, H., Functional oestrogen receptor alpha imaging in endometrial carcinoma using 16alpha-[^{18}F]fluoro-17beta-oestradiol PET. *Eur. J. Nucl. Med. Mol. Imaging* **2011,** *38* (1), 37-45.

14. van Kruchten, M.; Glaudemans, A. W.; de Vries, E. F.; Beets-Tan, R. G.; Schroder, C. P.; Dierckx, R. A.; de Vries, E. G.; Hospers, G. A., PET imaging of estrogen receptors as a diagnostic tool for breast cancer patients presenting with a clinical dilemma. *J. Nucl. Med.* **2012,** *53* (2), 182-90.

15. Zhao, Z.; Yoshida, Y.; Kurokawa, T.; Kiyono, Y.; Mori, T.; Okazawa, H., ^{18}F-FES and ^{18}F-FDG PET for differential diagnosis and quantitative evaluation of mesenchymal uterine tumors: correlation with immunohistochemical analysis. *J. Nucl. Med.* **2013,** *54* (4), 499-506.

16. Gemignani, M. L.; Patil, S.; Seshan, V. E.; Sampson, M.; Humm, J. L.; Lewis, J. S.; Brogi, E.; Larson, S. M.; Morrow, M.; Pandit-Taskar, N., Feasibility and predictability of perioperative PET and estrogen receptor ligand in patients with invasive breast cancer. *J. Nucl. Med.* **2013,** *54* (10), 1697-702.

17. Peterson, L. M.; Kurland, B. F.; Schubert, E. K.; Link, J. M.; Gadi, V. K.; Specht, J. M.; Eary, J. F.; Porter, P.; Shankar, L. K.; Mankoff, D. A.; Linden, H. M., A phase 2 study of 16alpha-[18F]-fluoro-17beta-estradiol positron emission tomography (FES-PET) as a marker of hormone sensitivity in metastatic breast cancer (MBC). *Mol. Imaging Biol.* **2014,** *16* (3), 431-40.

18. Allott, L.; Smith, G.; Aboagye, E. O.; Carroll, L., PET Imaging of Steroid Hormone Receptor Expression. *Mol Imaging* **2015,** *14*, 11-22.

19. Mankoff, D. A.; Tewson, T. J.; Eary, J. F., Analysis of blood clearance and labeled metabolites for the estrogen receptor tracer [F-18]-16 alpha-fluoroestradiol (FES). *Nucl. Med. Biol.* **1997,** *24* (4), 341-8.

20. Dehdashti, F.; Laforest, R.; Gao, F.; Aft, R. L.; Dence, C. S.; Zhou, D.; Shoghi, K. I.; Siegel, B. A.; Katzenellenbogen, J. A.; Welch, M. J., Assessment of Progesterone Receptors in Breast Carcinoma by PET with 21-(18)F-Fluoro-16 α ,17 α -[(R)-(1′ - α -furylmethylidene) Dioxy]-19-Norpregn-4-Ene-3,20-Dione. *J. Nucl. Med.* **2012,** *53* (3), 363-70.

21. Fowler, A. M.; Chan, S. R.; Sharp, T. L.; Fettig, N. M.; Zhou, D.; Dence, C. S.; Carlson, K. E.; Jeyakumar, M.; Katzenellenbogen, J. A.; Schreiber, R. D.; Welch, M. J., Small-animal PET of steroid hormone receptors predicts tumor response to endocrine therapy using a preclinical model of breast cancer. *J. Nucl. Med.* **2012,** *53* (7), 1119-26.

22. Chan, S. R.; Fowler, A. M.; Allen, J. A.; Zhou, D.; Dence, C.; Sharp, T.; Fettig, N. M.; Dehdashti, F.; Katzenellenbogen, J. A., Longitudinal Noninvasive Imaging of Progesterone Receptor as a Predictive Biomarker of Tumor Responsiveness to Estrogen Deprivation Therapy. *Clin. Cancer Res.* **2014**.

23. Fensome, A.; Bender, R.; Chopra, R.; Cohen, J.; Collins, M. A.; Hudak, V.; Malakian, K.; Lockhead, S.; Olland, A.; Svenson, K.; Terefenko, E. A.; Unwalla, R. J.; Wilhelm, J. M.; Wolfrom, S.; Zhu, Y.; Zhang, Z.; Zhang, P.; Winneker, R. C.; Wrobel, J., Synthesis and Structure-Activity

Relationship of Novel 6-Aryl-1,4-dihydrobenzo[d][1,3]oxazine-2-thiones as progesterone receptor modulators leading to the potent and selective nonsteroidal progesterone receptor agonist tanaproget. *J. Med. Chem* **2005,** *48,* 5092 - 5095.

24. Zhou, H.-B.; Lee, J. H.; Mayne, C. G.; Carlson, K. E.; Katzenellenbogen, J. A., Imaging Progesterone Receptor in Breast Tumors: Synthesis and Receptor Binding Affinity of Fluoroalkyl-Substituted Analogues of Tanaproget. *J. Med. Chem.* **2010,** *53* (8), 3349-3360.

25. Lee, J. H.; Zhou, H. B.; Dence, C. S.; Carlson, K. E.; Welch, M. J.; Katzenellenbogen, J. A., Development of [F-18]fluorine-substituted Tanaproget as a progesterone receptor imaging agent for positron emission tomography. *Bioconjug Chem* **2010,** *21* (6), 1096-104.

26. Pomper, M. G.; Katzenellenbogen, J. A.; Welch, M. J.; Brodack, J. W.; Mathias, C. J., 21-[^{18}F]fluoro-16.alpha.-ethyl-19-norprogesterone. Synthesis and target tissue selective uptake of a progestin receptor-based radiotracer for positron emission tomography. *J. Med. Chem.* **1988,** *31* (7), 1360-1363.

27. Buckman, B. O.; Bonasera, T. A.; Kirschbaum, K. S.; Welch, M. J.; Katzenellenbogen, J. A., Fluorine-18-labeled progestin 16.alpha.,17.alpha.-dioxolanes: development of high-affinity ligands for the progesterone receptor with high in vivo target site selectivity. *J. Med. Chem.* **1995,** *38* (2), 328-337.

28. Witney, T. H.; Alam, I. S.; Turton, D. R.; Smith, G.; Carroll, L.; Brickute, D.; Twyman, F. J.; Nguyen, Q. D.; Tomasi, G.; Awais, R. O.; Aboagye, E. O., Evaluation of deuterated 18F- and 11C-labeled choline analogs for cancer detection by positron emission tomography. *Clin. Cancer Res.* **2012,** *18* (4), 1063-72.

29. Haywood, T.; Kealey, S.; Sanchez-Cabezas, S.; Hall, J. J.; Allott, L.; Smith, G.; Plisson, C.; Miller, P. W., Carbon-11 radiolabelling of organosulfur compounds: (11) C synthesis of the progesterone receptor agonist tanaproget. *Chemistry* **2015,** *21* (25), 9034-8.

30. Yang, CP.; Cohen, D.; Greenberger, L. M.; Hsu, S. I.; Horwitz, S. B.; Differential transport properties of two mdr gene products are distinguished by progesterone, *J Biol Chem.* **1990** , *265* (18), 10282-8.

31. Jehangir, M.; Donald, A.; Alan, K.; Israel, H., Neurochemistry of Aging. 2. Design, Synthesis and Biological Evaluation of Halomethyl Analogues of Choline with High Affinity Choline Transport Inhibitory Activity. *J. Med. Chem* **1991,** *24,* 2031 - 2036.

32. Seo, J. W.; Chi, D. Y.; Dence, C. S.; Welch, M. J.; Katzenellenbogen, J. A., Synthesis and biodistribution of fluorine-18-labeled fluorocyclofenils for imaging the estrogen receptor. *Nuclear Medicine and Biology 34* (4), 383-390.

33. Pike, V. W., PET radiotracers: crossing the blood-brain barrier and surviving metabolism. *Trends Pharmacol Sci* **2009,** *30* (8), 431-40.

34. Smith, G.; Carroll, L.; Aboagye, E. O., New frontiers in the design and synthesis of imaging probes for PET oncology: current challenges and future directions. *Mol Imaging Biol* **2012,** *14* (6), 653-66.

35. Workman, P.; Aboagye, E. O.; Balkwill, F.; Balmain, A.; Bruder, G.; Chaplin, D. J.; Double, J. A.; Everitt, J.; Farningham, D. A.; Glennie, M. J.; Kelland, L. R.; Robinson, V.; Stratford, I. J.; Tozer, G. M.; Watson, S.; Wedge, S. R.; Eccles, S. A., Guidelines for the welfare and use of animals in cancer research. *Br. J. Cancer* **2010,** *102* (11), 1555-77.